

CO3-1 Development on In-Reactor Observation System Using Cherenkov Light

K. Tsuchiya, S. Kitagishi, Y. Nagao, N. Takemoto, M. Naka, A. Kimura, T. Sano¹, H. Unezaki¹, T. Yoshimoto¹, K. Nakajima¹, Y. Fujiwara¹, Y. Okumura¹ and S. Yamamoto¹

Neutron Irradiation and Testing Reactor Center, JAEA
¹Research Reactor Institute, Kyoto University

INTRODUCTION: The Cherenkov light is a faint emission accompanying the passage of charged particles through a transparent medium at speeds faster than the speed of light in that medium[1]. Since high-energy gamma rays can generate high-velocity electrons by Compton scattering, Cherenkov light can be emitted as a result of gamma radiation fields as well. Thus, the Cherenkov Viewing Device (CVD) was developed as an instrument specifically designed to form an image of the UV portion of this glow and it is used routinely by the IAEA around the world[2] to verify irradiated fuel stored at light-water reactor sites as well as at separate fuel storage facilities. In JMTR, the Cherenkov light from the spent fuels was measured by the video camera and correlation between gamma ray and illuminance was evaluated[3]. In this study, we are developing the in-reactor observation system for the management of reactor operation to establish the evaluation method of reactor power from the illuminance measurement of Cherenkov light.

EXPERIMENTS: The observation system of Cherenkov light is composed of the zoom camera with superHAD CCD, the controller of camera and the recorder. As the preliminary examinations, the measurement of illuminance for the diaphragm of camera and the selection of neutral density filters (ND-filters) with halogen light were carried out. Eight kinds of ND-filters were prepared in the experiments. The obtained data were evaluated by the image processing software called "Image J". From the

results of preliminary tests, the observation system of Cherenkov light for KUR (see Fig. 1) was established.

RESULTS: The relationship of transmittance between the catalogue value and measured value of the ND-filters is shown in Fig.2. From the result, the transmittance of the ND-filters up to 1/64 (ca. 1.5%) was the same as that of the catalogue value. On the other hand, the ND-filters with low transmittance were not agreed, and it is necessary to obtain the experimental data of transmittance with Cherenkov light. The analysis of transmittance by the Image J is shown in Fig.3. In this experiment, the illuminance was 1720lx and the ND-filter of 1/64 was used. The diaphragms of camera were F16 and F11. From the result, the analysis value of transmittance was about 0.37 and this value was different from the experimental data "0.47". It seems that the wavelength effects on the transmittance.

CONCLUSION: The observation system of Cherenkov light was established for the operating reactors, and the preliminary experiments were carried out to measure the illuminance with the halogen light. Properties on transmittance of the ND-filters were obtained. It is necessary to improve the analysis method of transmittance by the Image J. In future, the measurement of Cherenkov light inside the KUR core tank will be carried out with this observation system and correlation between illuminance of Cherenkov light and reactor power will be evaluated.

REFERENCES:

- [1] J.V. Jelley, Cherenkov Radiation and its Applications (Pergamon, New York, 1958).
- [2] E.M. Attas, J.D. Chen and G.J. Young, Nucl. Instr. and Meth. A 299(1990)88.
- [3] S. Watahiki, M. Nakamichi, et al., Annual meeting of Atomic Energy Society of Japan (2007).

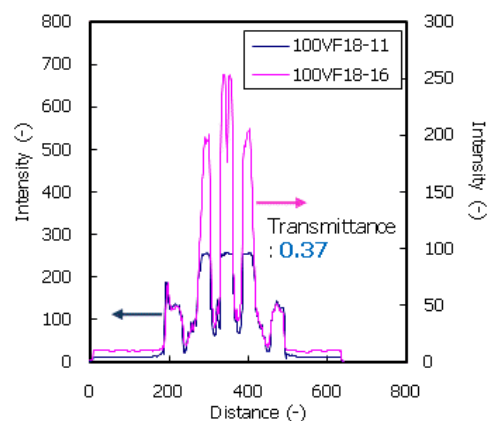
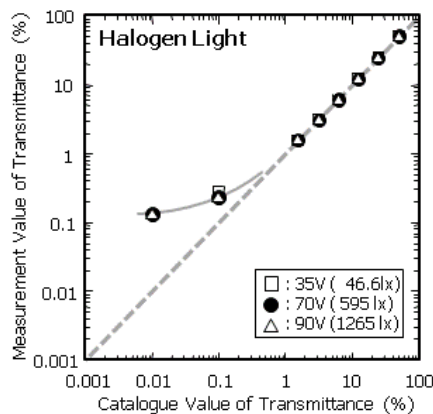
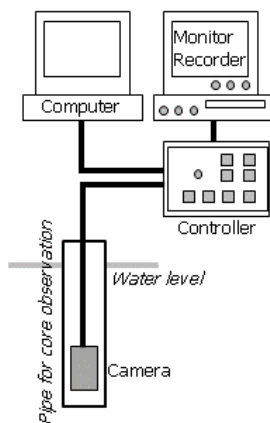


Fig.1. Concept of observation system of Cherenkov light in KUR

Fig.2. Relationship of transmittance between the catalogue value and measuring value of ND-filters

Fig.3. Analysis of transmittance by the Image J (Illuminance : 1720 lx, ND-filter : 1/64).

CO3-2 Development of Subcriticality Measurement for Accelerator-Driven Reactor (IV)

K. Hashimoto, H. Taninaka¹, A. Sakon¹, C. Pyeon², T. Misawa², T. Sano², H. Nakamura² and H. Unesaki²

Atomic Energy Research Institute, Kinki University
¹Interdisciplinary Graduate School of Science and Technology, Kinki University
²Research Reactor Institute, Kyoto University

INTRODUCTION: An accelerator-driven subcritical reactor system has been constructed in A-loading facility of the KUCA and a series of coherence-function measurement and Feynman- α analyses have been performed to develop the methodology of these subcriticality measurements. The preliminary results of coherence-function measurements are showed in this report.

EXPERIMENTS: These measurements were performed in a reactor system referred to as A3/8" P36EU(3). A tritium target was placed outside polyethylene reflector and pulsed neutron beam was emitted from the target. As pulsed beam frequency, 20, 100 and 500Hz were employed. Coherence function between two BF₃ counters closely placed were measured to determine the prompt-neutron decay constant. The experiments were carried out in two subcritical states. The subcriticality of the state was adjusted by changing control rod pattern. These control rod patterns are showed in Table 1.

Table 1. Control rod patterns employed

Pattern	Rod Position			Reactivity [% $\Delta k/k$]
	C1	C2, C3	S4~S6	
B	L.L.	L.L.	U.L.	-0.636
C	L.L.	L.L.	L.L.	-1.577

L.L.: Lower Limit, U.L.: Upper Limit

RESULTS: Figure 1 shows the coherence function measured for rod pattern B, where pulse frequency has set to 20Hz. Many sharp peaks were observed at integral multiple of pulse frequency 20Hz. In the case of pulse frequency of 100 and 500Hz, the peaks were appeared at integral multiple of the pulse frequency. Masking these peaks, the following equation was fitted to reduced data:

$$Coh(\omega) = \frac{A + B[1 + (\omega/\alpha_0)^2]}{A + 1 + (\omega/\alpha_0)^2}, \quad (1)$$

where ω is angular frequency(1/s), α_0 prompt-neutron decay constant, A and B constants related to reactor configuration and instrumentation system.

Figure 2 shows the reduced data and the fitted curve to the data. The least-squares fitting of Eq.(1) is successful. In Table 2, the prompt-neutron decay constant α_0 determined by the fitting are summarized. These decay-constants are consistent with that obtained by pulsed neutron method[1].

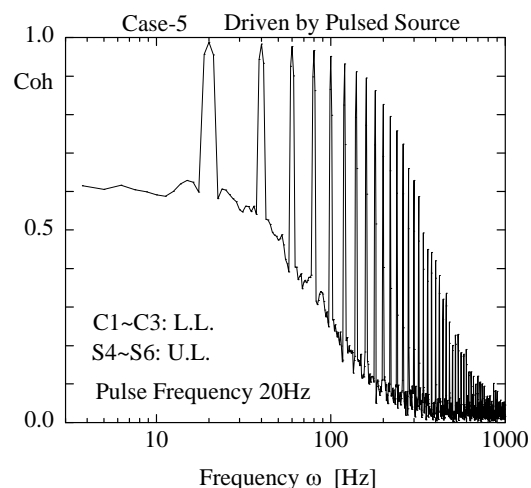


Fig. 1. Measured coherence function in pulse frequency of 20Hz

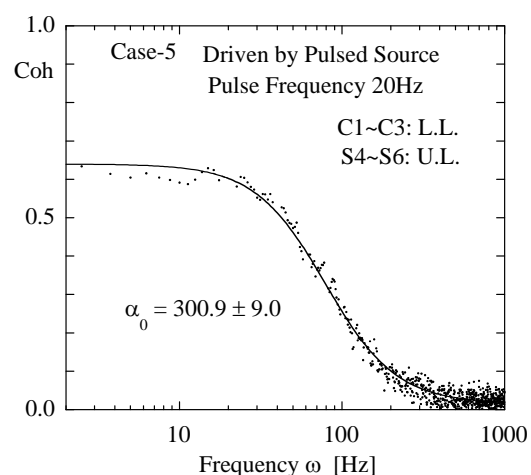


Fig. 2. Least-squares fit to measured coherence function in pulse frequency of 20Hz

Table 2. Prompt-neutron decay constant [1/sec]

Rod Pattern	Pulse Frequency[Hz]	Present	Pulsed Neutron Method
B	20	300.9 ± 9.0	303.9 ± 2.8
	100	310.6 ± 9.4	
	500	308.2 ± 9.0	
C	500	315.0 ± 9.4	506.8 ± 5.9
	500	488.5 ± 15.2	

tron method[1].

REFERENCES:

[1] H. Taninaka, K. Hashimoto, C. Pyeon, T. Sano, T. Misawa and T. Ohsawa, *J. Nucl. Sci. Technol.*, **47** (2010) 376-383.

K. Shimozato, K. Ieyama, T. Kitada, H. Okochi¹,
A. Yamamoto¹ and H. Unesaki²

Graduate School of Engineering, Osaka University
¹Graduate School of Engineering, Nagoya University
²Kyoto University Research Reactor Institute

INTRODUCTION: Rare-earth elements are considered as a candidate of advanced burnable poison. However, few critical experiments have been carried out so far to validate the accuracy of their nuclear data. So critical experiments loaded with rare-earth elements (Dy, Ho, Er and Tm) were carried out and their reactivity worth were measured at the KUCA B core. The experiments were performed on B3/8”P36EU(3) core and B1/8”P60EU-EU(5) core. These critical experiments attempt to estimate the validity of nuclear data of the rare-earth elements.

EXPERIMENTS: Preliminary experiment was carried out in June to determine the measured rare-earth elements, the arrangement of the core and the way of packing rare-earth elements into the core. We selected four elements to be measured: dysprosium (Dy), holmium (Ho), erbium (Er) and thulium (Tm) because these elements have sequential atomic numbers and consist a series of burnup chain. So it was considered that systematic data of these rare-earth elements would be expected. The rare-earth elements were used in the oxide form in the experiment because they are chemically stable. In addition, rare-earth elements has a large self-shielding effect caused by a large cross section, therefore the sample was diluted with alumina (Al₂O₃) powder to suppress the spatial self-shielding effect since Al₂O₃ has small impact on the excess reactivity. They were packed into an Al sample case (50.8mm × 50.8mm × 10.0mm), and the Al sample case was inserted at the center of fuel element (“sample fuel element”) as shown in Fig.1. The sample fuel element was loaded at the center of the core as shown in Fig.2. Figure 2 shows the arrangement of the two cores to be measured the sample worth. Two kinds of cores with different neutron spectrum (the B3/8”P36EU (3) core - softer spectrum, the B1/8”P60EU-EU(5) core - harder spectrum) were constructed to obtain the dependency of the sample worth on the neutron spectrum.

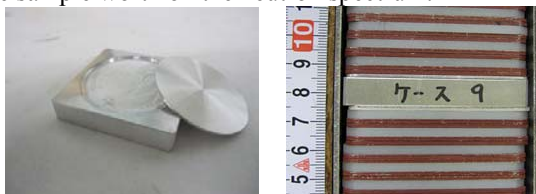


Fig.1. The packing of rare-earth elements (left): the loading of Al sample case to sample fuel element (right)

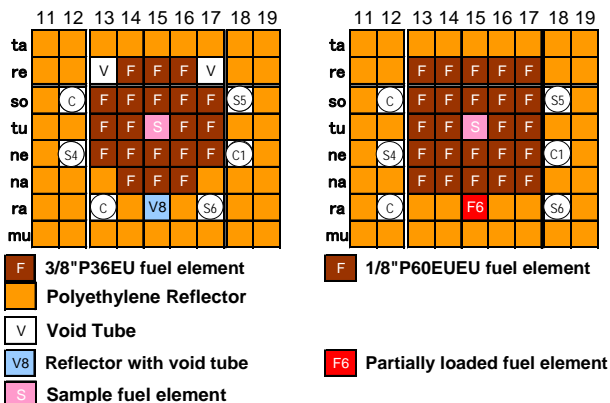


Fig.2. Arrangement of the two cores (left- B3/8”P36EU (3) core, right- B1/8”P60EU-EU(5) core)

On the basis of preliminary experiment, excess reactivity measurements of rare-earth sample were carried out in October. The special elements named “reflector with void tube” and “partially loaded fuel element” in Fig.2 were used to adjust the excess reactivity of the core to be approximately 0.25%Δk/k, and the reactivity worth of the rare-earth sample was adjusted to be approximately 0.15%Δk/k. The packing mass of rare-earth sample was determined through previous calculations by Monte-Carlo code MVP. First, the excess reactivity of the core with each sample was measured by the period method by changing the position of only C1 control rod. Then, we draw the reactivity curve of the C1 control rod to evaluate the excess reactivity of a core loaded with or without rare-earth sample by the position of C1 at critical point.

RESULTS: Table 1 shows the mass of each element in Al sample case and the average of sample worth on two cores. The number in parentheses is the number of the measurement. Sample worth of the rare-earth elements was evaluated with less than 0.01%Δk standard deviation from the difference of excess reactivity of the cores between with and without the rare-earth sample. The comparison of the sample worth between the measured results and the calculation results among the different nuclear libraries such as JENDL-3.3, ENDF/B-VII.0 and JEFF-3.1 is under execution.

Table 1. Sample worth of the rare-earth elements.

Core Type		Dy ₂ O ₃	Er ₂ O ₃	Ho ₂ O ₃	Tm ₂ O ₃
	mass (g)	0.95	9.00	3.50	6.00
B3/8”P36 EU (3)	sample worth (Δk/k)	0.174% (4)	0.185% (4)	0.161% (4)	0.172% (4)
	measurement error	(0.009%)	(0.004%)	(0.006%)	(0.004%)
	mass (g)	5.50	14.00	23.50	22.00
B1/8”P60 EU-EU(5)	sample worth (Δk/k)	0.138% (5)	0.151% (7)	0.119% (5)	0.141% (5)
	measurement error	(0.002%)	(0.004%)	(0.003%)	(0.006%)

K. Watanabe, A. Uritani, T. Tanabashi, C. Pyon¹ and T. Misawa¹

Graduate School of Engineering, Nagoya University
¹Research Reactor Institute, Kyoto University

INTRODUCTION: Real time neutron spectrometers have been desired to evaluate the performance of advanced nuclear facilities such as accelerator driven subcritical systems (ADS) and fusion reactors, which have intense and high energy neutron fields. We, therefore, proposed a novel neutron spectrometer which consists of multiple simple detectors having various threshold energies. The element detector of the proposed spectrometer consists of a radiator of recoil protons, a recoil proton stopping film and a thin scintillator for detection of protons passing through the stopping film, as shown in Fig. 1. The scintillation photons are transmitted through a light guide and detected by a photomultiplier tube. The maximum energy of recoil protons detected by the scintillator depends on the thickness of the stopping film. In other words, the threshold neutron energy of this detector E_{th} can be adjusted by varying the thickness of the stopping film. In addition, a thin scintillator results in low sensitivity for gamma-rays, because low LET fast electrons generated by gamma-rays pass through a scintillator without significant energy deposition. In this study, we discuss the fundamental properties of the element detector the proposed spectrometer through basic experiments and Monte Carlo simulations.

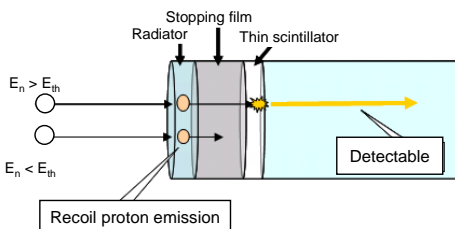


Fig. 1. Conceptual drawing of the element detector of on-line neutron spectrometer.

MONTE CALRO SIMULATIONS: The detail configuration of each element detector were designed by using Monte Carlo simulations. Figure 2 shows examples of the energy dependence of the detection efficiency for each element detector. The detection efficiencies with sharp thresholds and flat responses above the thresholds, which are well suited for the spectrum unfolding, were achieved by adjusting the thicknesses of the radiators and stopping films.

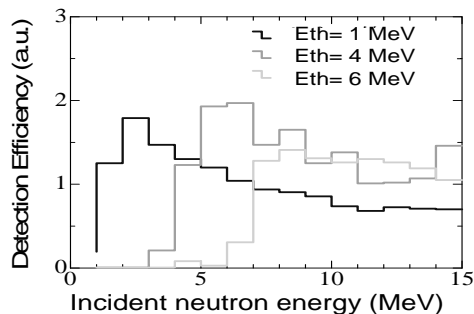


Fig. 2. Examples of the energy dependence of the detection efficiency for the detector with the threshold energy of 1, 4 and 6 MeV.

EXPERIMENTS: We made the basic experiments using the accelerator based DT neutron source at KUCA to confirm the fundamental performance of the proposed spectrometer. The six detectors with the threshold energies of 3, 5, 7, 9, 13 and 15 MeV were directly irradiated by the DT neutron source without neutron moderation. The DT neutron source were operated in the pulse mode with the pulse width of 25 μ s. These neutron pulses had after pulse components due to arc discharge ion source properties. The temporal detector responses are shown in Fig. 3. We confirmed that the detector with the threshold energy less than 14 MeV, which is the energy of DT neutrons, selectively had large response. The detector with the threshold energy of 15 MeV also responded because the energy threshold became unclear with increasing the threshold energy setting. These detectors were confirmed to have sufficient time response for ADS experiments.

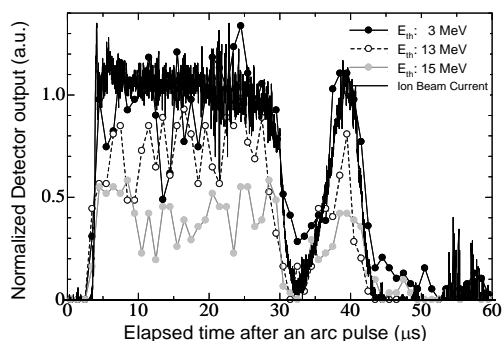


Fig. 3. Temporal detector responses for the detectors with the threshold energy of 3, 13 and 15 MeV. The DT neutron source was operated by the pulse mode with pulse width of 25 μ s. Temporal variation of the ion beam current of the DT source is also plotted.

CO3-5 Quantification of Neutron and γ Ray Fields for Subcriticality Determination (2)

Y. Nauchi, T. Kameyama, H. Unesaki¹, T. Misawa¹, T. Sano¹ and T. Yagi²

Central Research Institute of Electric Power Industry

¹Research Reactor Institute, Kyoto University

²Graduate School of Energy Science, Kyoto University

INTRODUCTION: In order to observe linear relation between the subcritical multiplication factor k_{sub} and yield ratio of γ rays to neutrons, measurement techniques of total yields of both radiations have been studied. Measurements of fission γ rays and neutron absorptions outside subcritical cores had been conducted.

EXPERIMENTS: 4 subcritical cores which consist of C35 assemblies (4, 3, 2 rows x 2 columns and 2 rows x 1.5 column) were mocked up as shown in Fig. 1. Those cores were driven by a ²⁵²Cf source of 1.3×10^6 Bq inserted near the core center. To obtain axial fission distribution, Indium (In) wires of 1.5 mm diameter is irradiated in the cores. The γ ray spectra were measured with a BGO scintillator (BGO) located at 36cm outside the cores. 2.223MeV γ rays emitted from H(n, γ) reactions in water outside the cores were measured with a NaI scintillator (NaI) shielded by a Pb shadow bar eliminating the direct γ rays originated in the cores. Measurements with BGO and NaI were also performed for a ²⁵²Cf with no fuel case. H(n, γ) reaction distributions were experimentally evaluated assuming equivalence of them to those of ⁶Li(n,t) and ¹¹⁵In(n, γ) reactions. Then we measured neutrons with three ⁶Li fiber scintillator detectors (horizontal direction) and In wires activation (axial direction) by applying more intense ²⁵²Cf source (6.2×10^6 Bq).

RESULTS: The measured γ ray pulse height spectra in BGO consist of fission and capture components [1]. Pulse counting of fission γ rays was simulated with MCNP-5 taking into account of axial fission distributions evaluated by the measured activities of the In wires irradiated in the cores. Horizontal distributions of fission were modeled by cosine shape functions as done by Suzuki [2]. Primary and secondary fission γ ray yields were estimated by normalizing the calculated pulse height spectra to the measured fission ones in BGO for the four cores and the no fuel geometry. With the data of yield ratio of γ ray to neutron [3], the primary and the secondary neutron yields were estimated separately. Finally, k_{sub} s were deduced. The values agree with ones by neutronics calculations as listed in Table 1, which confirms the measurements technique of total fission γ ray yield.

With NaI, 2.223MeV γ rays in H(n, γ) reactions were measured. Pulse counting of γ rays with NaI was simulated by coupled neutron – photon transport calculations with MCNP-5. The calculated count rates are compared to the measured ones in Table2. The fractional standard deviation of C/E for the 5 geometries is 5.1%.

Contributions of the H(n, γ) reactions in the water outside the cores to the 2.223MeV γ ray count rates

in NaI were estimated by the measured ⁶Li(n,t) reaction rates multiplied by detection efficiency evaluated by photon transport calculation with MCNP-5. As shown in Fig. 2, significant contribution is still found in points near the NaI, although ⁶Li(n,t) reaction rates is low. For quantification of neutron absorption outside the core by measured count rates with NaI and the Li fibers without neutronics calculations, the H(n, γ) reactions occurring near the NaI should be reduced.

REFERENCES:

- [1] Nauchi *et al.*, KURRI progress report., (2008) C03-5.
 [2] Suzuki, *et al.*, Preprints 2002 Ann. Meeting of At. Energy Soc. of Jpn., Iwaki, Japan, Sep 14–16, (2002), I12.
 [3] J.M.Verbeke *et al.*, UCRL-AR-228518, 2009.

Table 1. k_{sub} evaluated by γ ray (3.0-4.5MeV) count rates in BGO in comparison to neutronics calculation.

Core	2x1.5	2x2	3x2	4x2
k_{sub} by γ ray measurement	0.699	0.786	0.898	0.959
error	0.007	0.007	0.010	0.011
k_{sub} by calculation.	0.726	0.792	0.897	0.956

Table 2. Photo-electric peak counts for H(n, γ) γ ray in NaI.

Core	0	2x1.5	2x2	3x2	4x2
Measured(cps)	9.307	1.043	1.207	1.980	6.897
err	0.012	0.013	0.012	0.011	0.005
MCNP($\times 10^{-6}$)	69.5	7.28	9.15	13.9	46.1
rel. err	0.012	0.019	0.023	0.030	0.023
E/C($\times 10^5$)	1.34	1.43	1.32	1.42	1.50

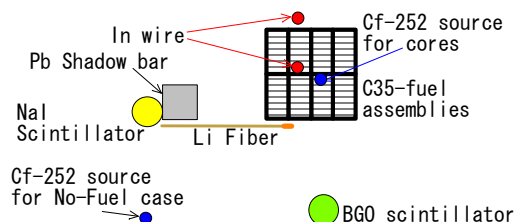


Fig. 1. Geometry of subcritical measurement.

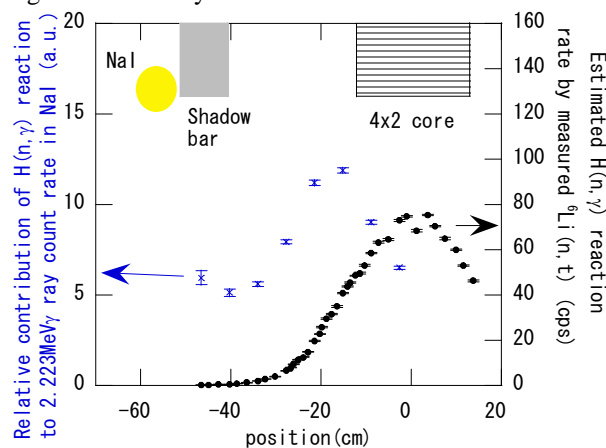


Fig. 2. H(n, γ) reaction distribution evaluated by ⁶Li(n,t) count rate (black dots) and contribution of H(n, γ) reaction to 2.223MeV count rate in the NaI (blue cross).

K. Nishihara, T. Sugawara, K. Tsujimoto, Y. Kitamura and C. H. Pyeon¹

Japan Atomic Energy Agency

¹Research Reactor Institute, Kyoto University

INTRODUCTION: The regression method for pulse neutron source (PNS) experiment was developed in Ref[1] to monitor sub-criticality of an accelerator-driven system (ADS). This method is applicable to PNS experiment with poor experimental conditions, such as high pulse repetition frequency of neutron source that makes the alpha-fitting method difficult to determine the delayed neutron level.

In the present study, the regression method was verified using the KUCA-A core with various sub-critical levels induced by DT neutrons with several numbers of pulse repetition frequencies.

EXPERIMENTS: A BF₃ counter was set beside the core with a DT neutron source. Three subcritical cores with different positions of the control and safety rods were employed (Table 1). Frequency of the DT neutron source was varied from 10 to 800 Hz, where the frequency less than 50 Hz is normally adopted for the alpha fitting method.

REGRESSION METHOD: The next formula is derived from one-point dynamic equation and a periodic boundary condition.

$$n(t; S_0, \rho) = S_0 \left\{ \frac{1}{l} \frac{1}{1 - e^{-\alpha l}} e^{-\alpha t} + \frac{1}{\rho - \beta} \frac{\beta}{\rho} f \right\}, \alpha = -(\rho - \beta)/l$$

Here, $n(t)$ is a time evolution of counting rate from a detector, S_0 a variable for normalization, l an average lifetime of neutrons, f a pulse repetition frequency of DT source, ρ ($=1-1/k_{eff}$) a reactivity, and β a ratio of delayed neutrons.

We fitted this formula to experimental results and obtained the most likely values and errors of S_0 and ρ considering statistic error of the counters.

RESULTS: Figure 1 shows experimental results by rod-worth method, regression method and alpha-fitting method. A large discrepancy was observed for the regression method with 10 and 25Hz, while the alpha-fitting method agrees well to the rod worth method. Figure 2 shows counting rates for the frequency of 25Hz with those estimated by the regression method. The influence of higher modes at the beginning of measurement was eliminated by adopting the regression analysis from 1.5 ms. The reason of discrepancy between experiment and the regression method was supposed to be an existence of background, which is expected to be around 800 counts per second (100 counts per channel) from the analysis of Fig. 2.

CONCLUSION: The regression method was investigated for the wide range of DT neutron source frequency. The discrepancy of k_{eff} and count rates between experi-

ment and the regression method was observed for the low frequencies. Further investigation for background is necessary in the next study.

REFERENCE:

[1] K. Nishihara, *et. al.*, "Pulse Neutron Experiment for Accelerator-Driven System," *KURRI PROGRESS REPORT 2007*, CO3-4 (2007).

Table 1. Conditions of the PNS experiment.

Frequency (Hz)	10, 25, 100, 250, 800		
Counters	BF ₃		
Core Index	Core A	Core B	Core C
CR position	CR1 full in	CR1, CR2 and CR3 full in	All CRs and SRs full in
k_{eff} (rod worth)	0.9956	0.9916	0.9823
β_{eff}^*	0.00802	0.00812	0.00813
l (sec)*	5.392E-05	5.300E-05	5.084E-05

* calculated by MCNP code

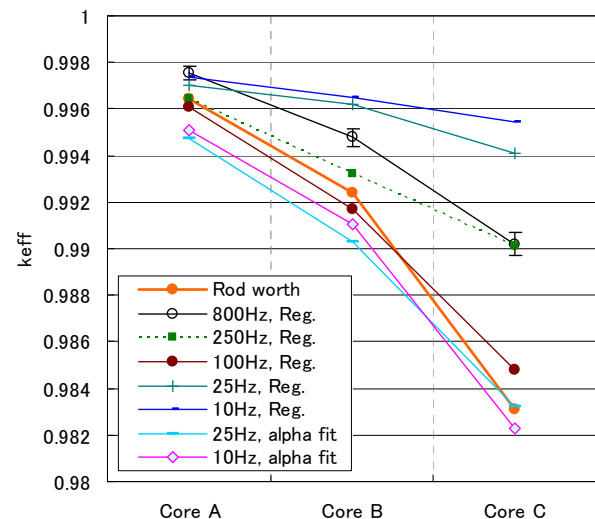


Fig. 1. k_{eff} by rod worth, regression method, and alpha-fitting method.

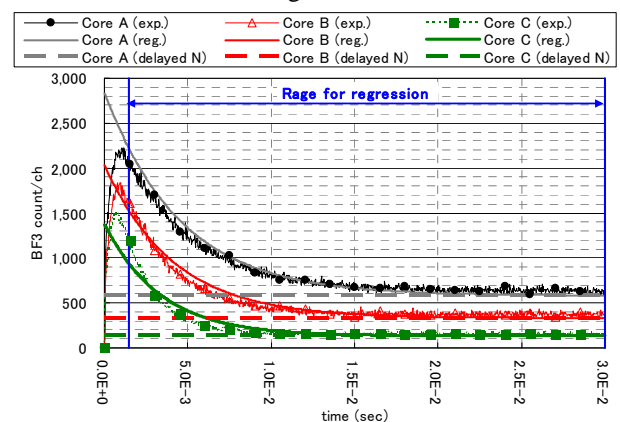


Fig. 2. Experimental result (25Hz).